Earth Planets Space, **51**, 1145–1151, 1999

Constrained inversion of COPROD-2S2 dataset using model roughness and static shift norm

Yasuo Ogawa

Geological Survey of Japan, 1-1-3 Higashi, Tsukuba, Ibaraki 305-8567, Japan

(Received November 7, 1998; Revised May 11, 1999; Accepted May 11, 1999)

A two-dimensional inversion method was applied to the COPROD-2S2 dataset, which consists of apparent resistivity, phase, and magnetic transfer functions at 33 sites over 3.5 decade period band. The modeling procedure adjusts tradeoff between the data misfit, model roughness and static shift L2 norm. Two different models were made using strong and weak constrains on the shallower structure than the typical shortest skin depth (1.5 km). Stronger constraint on the shallow horizontal roughness lead to larger static shifts in TM mode and horizontally smoother structure. This shows tradeoff between the shallow resistivity roughness and static shift in TM mode. However, both models had consistent features in the deep resistivity structure and the static shift in TE mode. Both models showed consistent results on the background structures, which were estimated by the resistivity blocks outside the data area.

1. Introduction

The COPROD-2S2 is an artificial magnetotelluric dataset prepared by Ivan Varentsov. One of the purposes of distributing this dataset is to diagnose two-dimensional inversion codes. This dataset was created by a forward modeling responses of an unknown specific model, which were then contaminated with random noise, outliers and static shifts. This dataset is available from the web sites (http://user.transit.ru/~igemi/c_2s_p0.html or http://www.cg.NRCan.gc.ca/mtnet/coprod2s.html). Thus this data set gives an excellent opportunity to check the result with the true model. Specifically, the focus is put upon whether or not the background one-dimensional structure as well as the spatial distribution of the true resistivity is recovered.

There are 33 sites along a 50 km long profile. The period range is 3.5 decades wide. There are 8 periods ($T = 1, 3, 10, 30, 100, 300, 1000, 3000$ s). At each site, there are TE and TM responses. Apparent resistivity and impedance phase are available in both modes. Magnetic transfer functions are also available.

Static shift gives an upward or downward parallel shift of apparent resistivity curve in a log(period) versus log(apparent resistivity) plot (Jones, 1988). Static shift distorts only the apparent resistivity curves. Static shift is a function of sites and modes. In this paper, the static shift g is defined as follows:

$$g_{site,mode} = \log_{10} \rho_a^{obs} - \log_{10} \rho_a^{undist}. \tag{1}$$

Here, ρ_a^{obs}, and ρ_a^{undist} are observed (COPROD-2S2) and undistorted(static shift removed) apparent resistivity, respectively.

It is necessary to have another independent information or an assumption to remove the static shift from the MT dataset. If there is a priori information on the shallow or deep structure, static correction can be done explicitly. Time domain sounding using magnetic fields can help estimate the undistorted shallow structure (Sternberg *et al.*, 1988). Global resistivity distribution by deep geomagnetic depth sounding (GDS) can help to estimate the long period asymptote. However, in this paper, no other information than the data itself was used. The assumption in this study is that the static shift follows Gaussian distribution. It is a very simple, but reasonable assumption.

2. Norms to Minimize

The process of the inversion is based on that of Ogawa and Uchida (1996). The basis of the idea will be described briefly.

The model was constructed using rectangular finite elements, which were grouped into regularization blocks (Fig. 1). The static shifts g were taken as model parameters as well. Therefore, the model parameters m are written as follows:

$$m = \begin{bmatrix} m_{\rho,block} \\ g_{site,mode} \end{bmatrix} \tag{2}$$

where $m_{\rho,block}$ denotes the $\log_{10}$(resistivity) of the regularization blocks. Model misfit is defined as follows:

$$S(m) = |Wd - WF(m)|^2 \tag{3}$$

where d, W, and F denote data, reciprocal of the standard error of the data, and function mapping a model into the data space, respectively. S can be approximated by S_0 as shown below using the model parameters of the previous iteration m_{old} and a Jacobian matrix A.

$$S(m) \approx S_0(m) = \left| W\tilde{d} - WAm \right|^2 \tag{4}$$

Copy right© The Society of Geomagnetism and Earth, Planetary and Space Sciences (SGEPSS); The Seismological Society of Japan; The Volcanological Society of Japan; The Geodetic Society of Japan; The Japanese Society for Planetary Sciences.

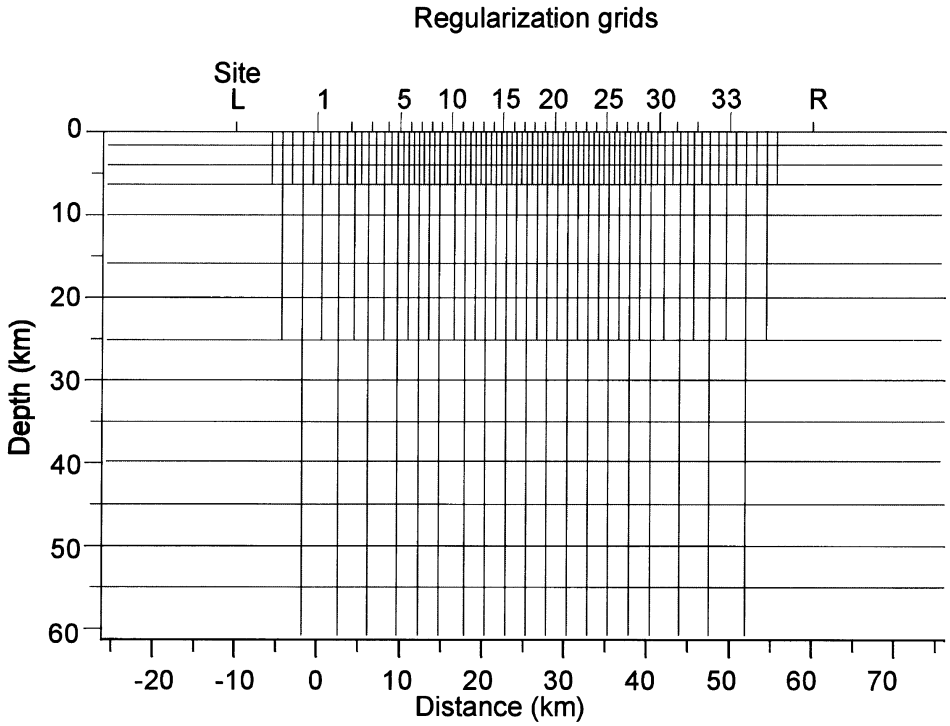

Fig. 1. Regularization grids for the two-dimensional inversion. Sites L and R are representative sites for background resistivity model.

where,

$$\tilde{d} = d - F(m_{old}) + Am_{old}. \tag{5}$$

S_0 (instead of S) was minimized under the constraints of minimizing the following two norms.

One is a model roughness norm and the other is the static shift L2 norm. Model roughness is defined as R as follows:

$$R = \left|C_v m_\rho\right|^2 + \left|C_h m_\rho\right|^2. \tag{6}$$

The first and second terms denote the vertical roughness and horizontal roughness, respectively. Matrix C_v is composed of coefficients so that the i-th row of $C_v m_\rho$ represents the difference between the $\log_{10}$(resistivity) of the i-th regularization block and the average of the neighboring vertical blocks. Likewise, Matrix C_h is composed of coefficients so that the i-th row of $C_h m_\rho$ represents the difference between the $\log_{10}$(resistivity) of the i-th regularization block and the average of the neighboring horizontal blocks.

The second norm is the static shift $L2$ norm, G, defined as follows:

$$G = \sum \left|g_{site,mode}\right|^2 \tag{7}$$

The constrained inversion will be formulated as minimizing the following U:

$$U = S_0 + \alpha^2 R + \beta^2 G \tag{8}$$

where α, and β are hyper parameters. Because of the linearization in Eq. (4), U is quadratic with respect to the model parameter m. Given proper α, and β, the model parameter m can be sought from the Eq. (8).

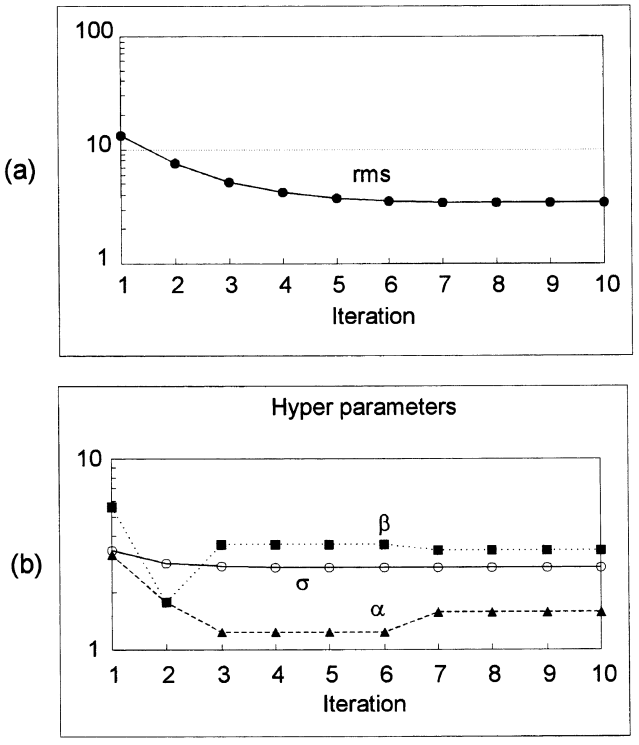

Fig. 2. (a) rms as a function of the iterations, (b) hyper parameters σ, α and β as functions of the iterations.

3. Proper Tradeoff between the Norms

The best combination of hyper parameters was determined by maximizing Bayesian likelihood (Akaike, 1980; Uchida, 1993a,b).

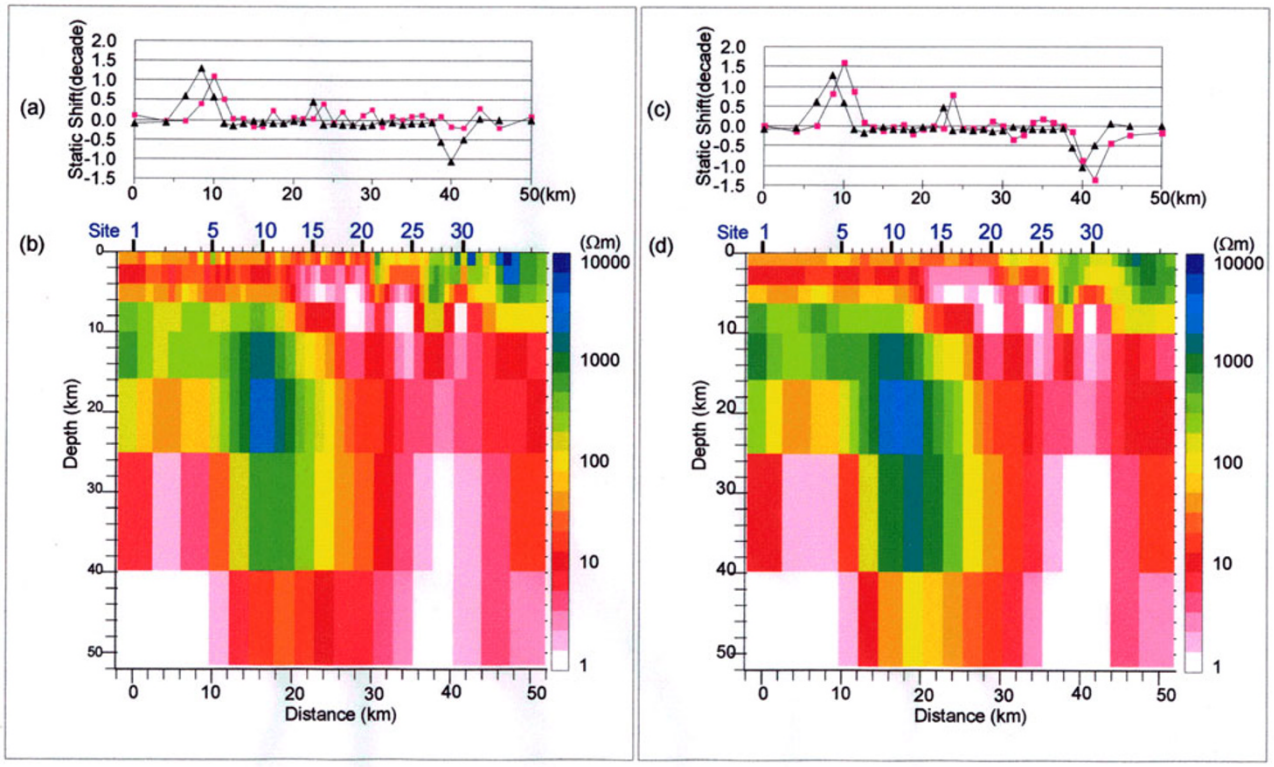

Fig. 3. (a) Distribution of static shift for the basic model. TM and TE mode static shifts are shown by pink squares and black triangles, respectively. (b) The basic model. (c) Distribution of static shift for the shallow horizontal model. (d) The shallow horizontal model.

In Bayesian statistics, the probability density function of the whole data d with regard to model m is as follows:

$$p(d|m) = \left(2\pi\sigma^2\right)^{-N/2} \exp\left(-\frac{S_0}{2\sigma^2}\right) \tag{9}$$

where N is the number of the data. σ is the standard deviation and should be one if the data error is properly estimated in Eq. (3). Thus σ can also be thought of as the correction factor to the estimated standard deviation.

Next, Gaussian distributions are assumed for the roughness of the model, and the static shift. Thus, the prior distribution of the model is as follows:

$$\pi(m) = D\left(2\pi\sigma^2\right)^{-N/2} \exp\left(-\frac{\alpha^2 R}{2\sigma^2} - \frac{\beta^2 G}{2\sigma^2}\right) \tag{10}$$

where D is a normalizing factor when $\pi(m)$ is integrated over the whole model space. The likelihood of the data is written as L which is a function of σ, α, and β:

$$L(\alpha, \beta, \sigma) = \int p(d|m)\pi(m)dm. \tag{11}$$

Note that both $p(d|m)$ and $\pi(m)$ have quadratic terms in the argument for their exponential and can be easily calculated (Ogawa and Uchida, 1996). Given α and β, L is maximized with the following σ:

$$\sigma^2 = \frac{1}{N} \min\left(S_0 + \alpha^2 R + \beta^2 G\right). \tag{12}$$

In order to maximize L value with respect to α and β, a direct numerical search (SYMPLEX method) was used.

Maximizing L is equivalent to minimizing Akaike's Bayesian Information Criterion (ABIC) (Akaike, 1980; Uchida, 1993a,b), which is defined as below:

$$ABIC(\alpha, \beta) = -2\log(\max L) + 2(dimension\ of\ hyper\ parameters). \tag{13}$$

After finding the three proper hyper parameters (α, β, and σ), new model parameters m will be determined by minimizing U in Eq. (8). Since the linearization is applied, the whole process must be iterated.

4. Application to COPROD-2S2 Dataset

The algorithm outlined above was applied to the COPROD-2S2 dataset. The whole dataset was used for the inversion, i.e., apparent resistivity, phase, magnetic transfer functions were used for the 33 sites at 8 frequencies. Both TE and TM mode were used.

Figure 1 shows the regularization grids used for the inversion. The shallowest regularization layer has a thickness of 1.6 km, which is comparable to the Bostick depth for the typical apparent resistivity (30 Ω·m) at the shortest period (1 s). Error floors were 5% for the apparent resistivity (also equivalent one for phase) and 0.05 for transfer functions. Because of the inherent non-linearity, new model parameters m_{new} was not determined directly by the predicted parameters $m_{predicted}$. The change of the models was done more slowly as follows.

$$m_{new} = m_{old} + r(m_{predicted} - m_{old}). \tag{14}$$

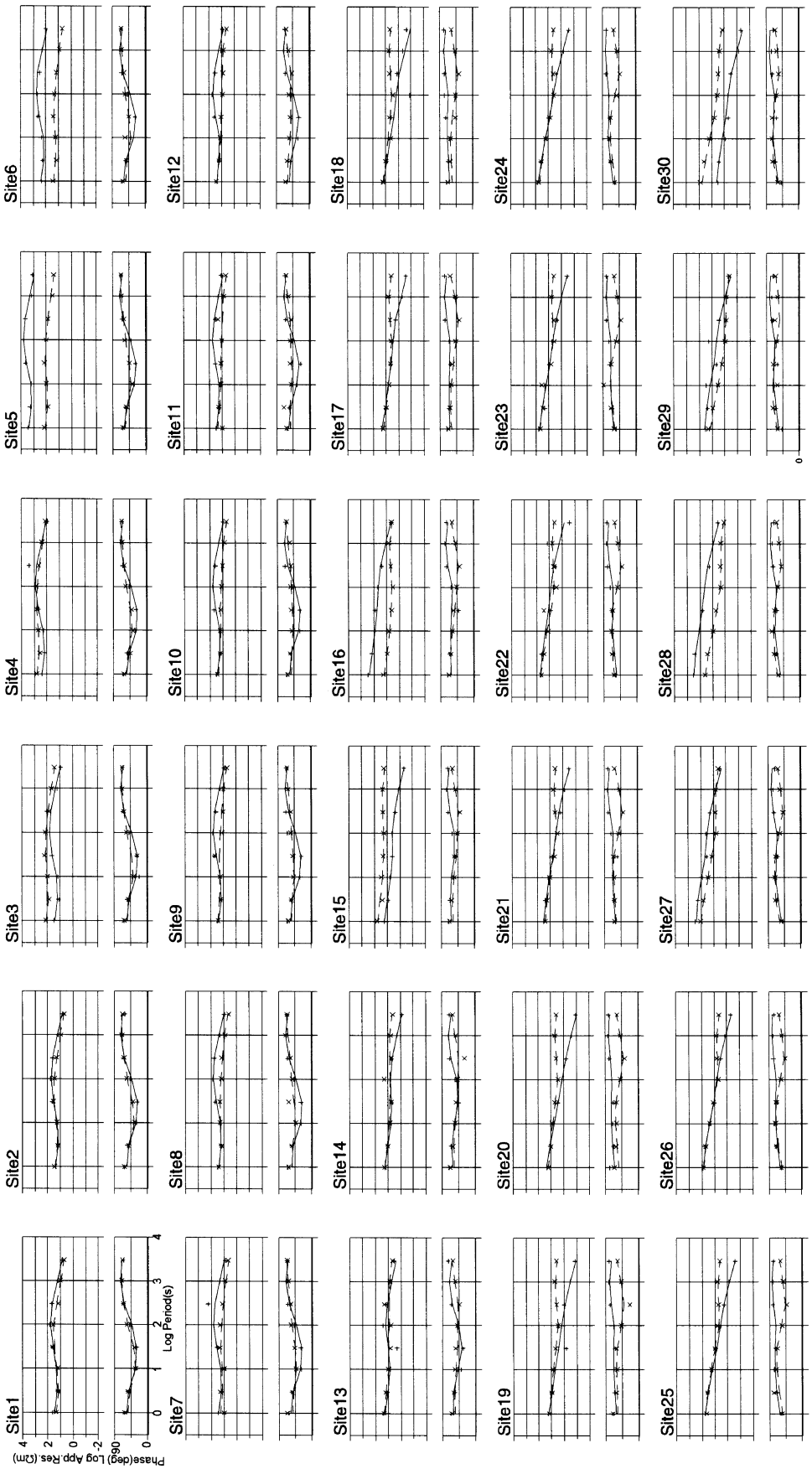

Fig. 4. Apparent resistivity and phase plots for the whole dataset. The plus and cross denote the observed data for TM and TE modes, respectively. The solid and broken lines denote the theoretical responses including static shifts for the TM and TE modes, respectively.

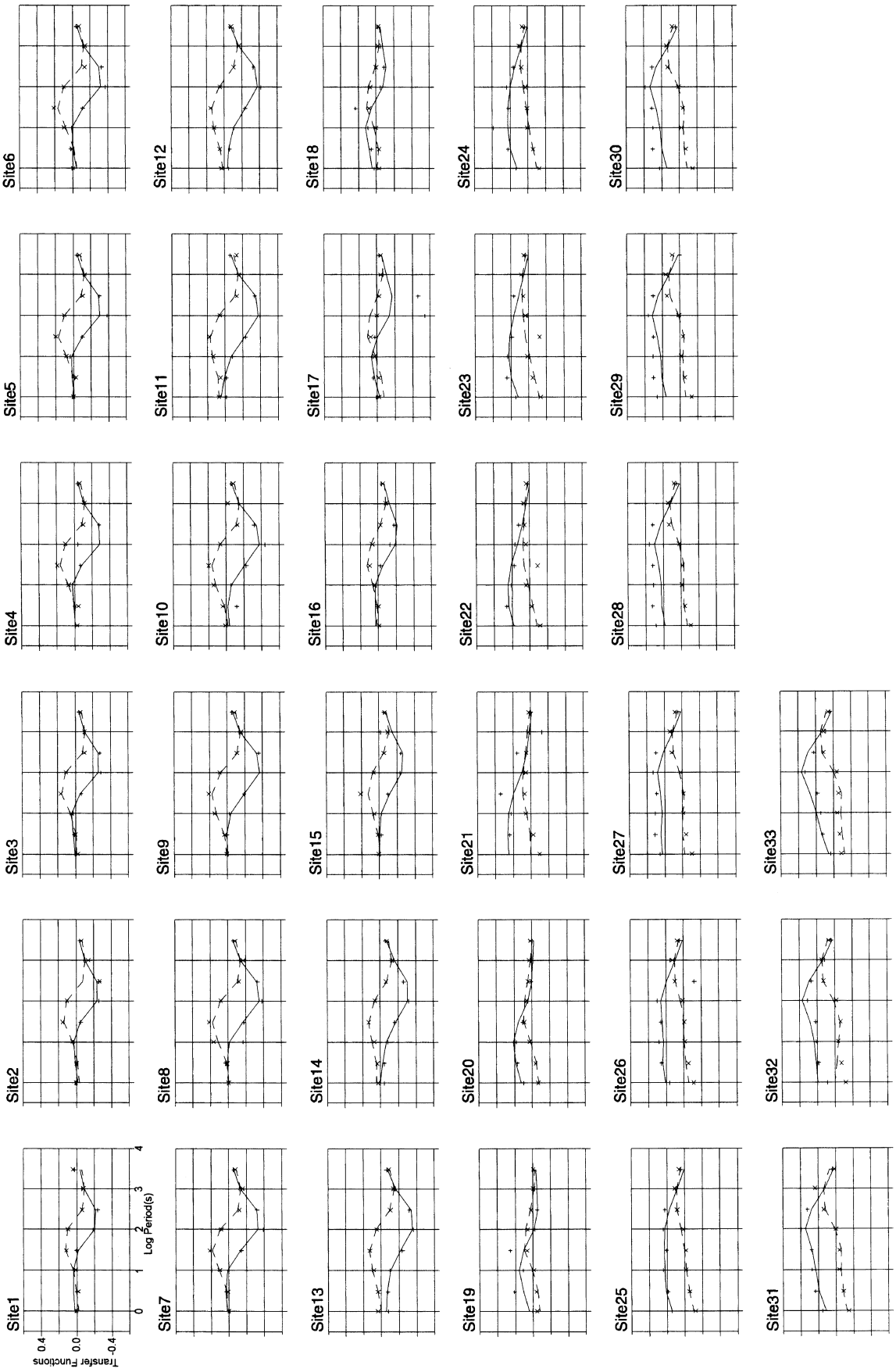

Fig. 5. Magnetic transfer function plots for the whole dataset. The plus and cross denote the observed data for real and imaginary parts, respectively. The solid and broken lines denote the theoretical responses for the real and imaginary parts.

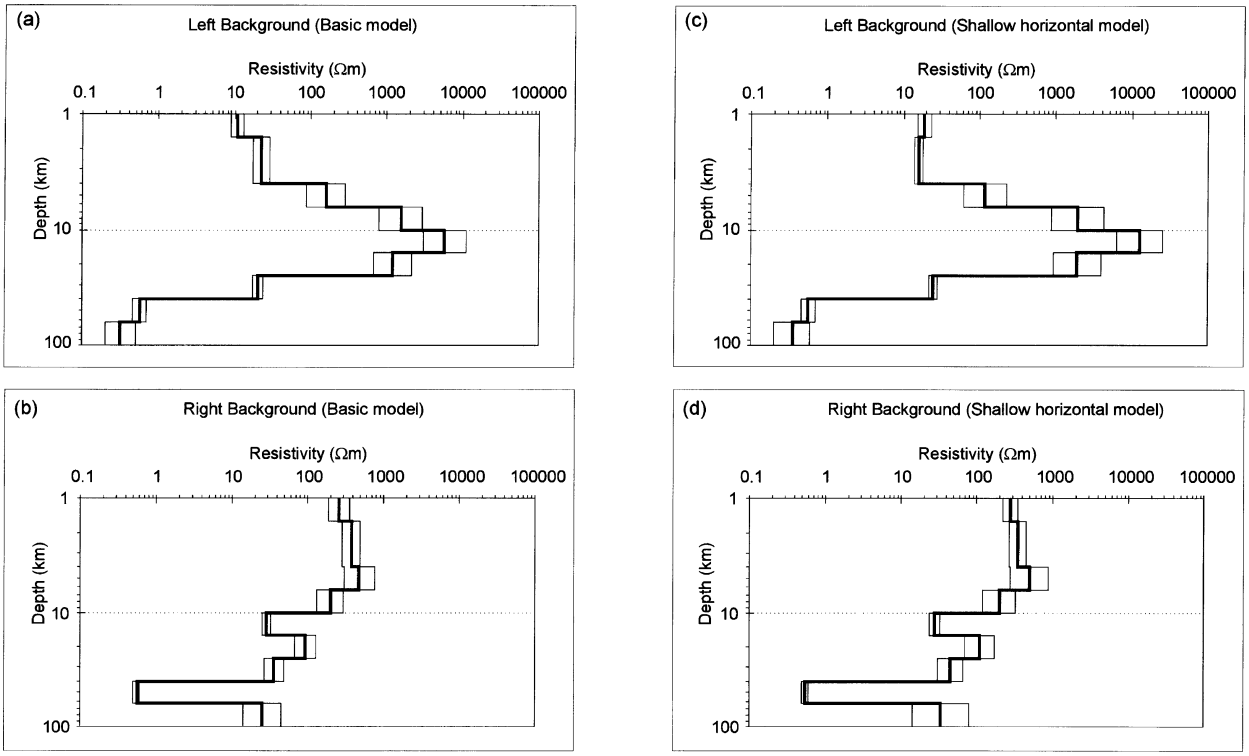

Fig. 6. One dimensional background resistivity models on both ends of the model. Left and Right background models were taken at sites L and R in Fig. 1. Left and right background model of the basic model (Fig. 3(b)) are shown in (a) and (b). Left and right background model of the shallow horizontal model (Fig. 3(d)) are shown in (c) and (d). The three lines in each figure means the average and one standard deviation of the estimated resistivity values.

Here r was set as 0.5 throughout the iterations.

After 10 iterations, the rms converged to 3.39 (Fig. 2(a)). The three hyper parameters also converged (Fig. 2(b)). The final σ was 2.7. As seen in Eqs. (4) and (9), it should be 1, if the data is properly scaled by its variance. From the algorithm, the proper error is 2.7 times more. This is representing that the data error itself is underestimated or that the data is biased by outliers.

Figures 3(a) and (b) illustrate distribution of static shift and the final model, respectively. The static shift is fairly small (less than 0.5 decade in magnitude) in the middle of the profile. Large static shifts were obtained at around 8.50 km (from 6.50 to 11.25 km), and around 40.0 km (from 38.75 to 41.50 km). Such locations have local complex resistivity structures at the top layer (Fig. 3(b)). The static shift is partly represented by the static shift parameters g, but still partly represented by the shallow structures. There is a tradeoff between the static shift and the model roughness, especially in the shallow part.

For comparison, stronger constraint was introduced for the roughness of the shallow structure. The coefficient C_h in the shallow (1.6 km) structure was multiplied by 10, while other C_v and C_h remained unchanged. This will give more penalty if the shallow structure is not horizontally smooth. Using this modified roughness, similar inversion was performed for ten iterations. Figures 3(c) and (d) illustrate distribution of static shift and the final model. As expected, the distinct shallow resistivity anomalies, which were evident in the Fig. 3(b), were smoothed out in Fig. 3(d). Static shifts in TE mode in Fig. 3(c) have similar distribution to the ones in Fig. 3(a). On the other hand, those of TM mode have larger amplitudes. One major difference lies in the static shift in TM mode at around 40 km, where original model (Fig. 3(b)) had high resistivity anomaly in the shallow depth. In Fig. 3(b), the top regularization block of site 30 (at 41.5 km) was sandwiched by two resistive blocks, which will help shift down the apparent resistivity curve in TM mode. On the other hand, in Fig. 3(d), the corresponding shallow structure is horizontally smoothed and the static shift parameters have larger amplitude.

Figure 4 shows the data fit for apparent resistivity and phase for the model in Figs. 3(a) and (b). Note here that the model response includes static shift. Figure 5 shows the data fit for magnetic transfer functions. As seen in Figs. 4 and 5, the model curves are fitting well to apparent resistivity, phase, and transfer function data.

Note here that regardless of the different structure at the first regularization block (1.6 km), the deeper structures are fairly consistent between the two models (Figs. 3(b) and (d)). Lastly, one-dimensional background structures were plotted as a function of depth on both sides of the two models. As shown in Fig. 1, the inversion included resistivity blocks outside the data area. The sites L and R in Fig. 1 represent regional sites. The structure beneath these sites were plotted as a function of depth. Figures 6(a) and (b) represent left and right regional models using the original roughness coefficient. Figures 6(c) and (d) represent left and right regional models where shallow structure is horizontally constrained. Aside from the top layer, which interacts with static shift strongly, both models gave the consistent results.

5. Conclusion

The COPROD-2S2 dataset was inverted by a two-dimensional technique using two constraints, roughness and static shift norm. The modeling procedure adjusts tradeoff between the data misfit, model roughness and static shift L2 norm. Two kinds of models were obtained using weak and strong constraints on the shallow horizontal roughness. The boundary between the shallow and deep structures was set at 1.6 km which corresponds to the Bostick depth for typical apparent resistivity (30 Ω·m) at the shortest period (1 s). Stronger constraint on the horizontal shallow (1.6 km) roughness lead to horizontally smoother structure at the shallow depth and larger static shift in TM mode. Tradeoff was evident between the shallow resistivity roughness and static shift in TM mode. However, both had consistent features in the deep resistivity structures and the static shift in TE mode. Background structure was investigated using the resistivity blocks outside the data area, which were also variables in the inversion. Both models had consistent background structures on both ends.

Acknowledgments. Ivan Varentsov and Alan Jones made COPROD-2S2 dataset available. This paper was presented at the fourth international Magnetotelluric data interpretation workshop (MT-DIW4), Sinaia, Romania, in August 1998, which was organized by Dumitru Stanica and Alan Jones.

References

Akaike, T., Likelihood and Bayes procedure, in *Bayesian Statistics*, edited by J. M. Bernardo, M. H. deGroot, D. V. Lindley, and S. F. Smith, pp. 143–166, University press, Valencia, 1980.

Jones, A. G., Static shift of magnetotelluric data and its removal in a sedimentary basin environment, *Geophys.*, **53**, 967–978, 1988.

Ogawa, Y. and T. Uchida, A two-dimensional magnetotelluric inversion assuming Gaussian static shift, *Geophys. J. Int.*, **126**, 69–76, 1996.

Sternberg, B. K., J. C. Washburne, and L. Pellerin, Correction for the static shift in magnetotellurics using transient electromagnetic soundings, *Geophys.*, **53**, 1459–1468, 1988.

Uchida, T., Smooth 2-D inversion for magnetotelluric data based on statistical criterion ABIC, *J. Geomag. Geoelectr.*, **45**, 841–858, 1993a.

Uchida, T., Inversion of COPROD2 magnetotelluric data by use of ABIC minimization method, *J. Geomag. Geoelectr.*, **45**, 1063–1071, 1993b.

Y. Ogawa (e-mail: oga@gsj.go.jp)